SHOCK-LIKE FOCUSING OF INERTIAL WAVES - THE LOCALIZED GENERATION OF TURBULENCE

Jie Liu
Chair of Fluid Dynamics,
Department of Mechanical Engineering
Technical University of Darmstadt
64287 Darmstadt, Germany
liu@fdy.tu-darmstadt.de

Ahmed Mohamed
Fluid mechanics and acoustics laboratory
Ecole Centrale de Lyon
69130 Ecully, France
ahmed.mohamed@ec-lyon.fr

Alexandre Delache
Fluid mechanics and acoustics laboratory
Ecole Centrale de Lyon
69130 Ecully, France
alexandre.delache@ec-lyon.fr

Fabien Godeferd
Fluid mechanics and acoustics laboratory
Ecole Centrale de Lyon
69130 Ecully, France
fabien.godeferd@ec-lyon.fr

Martin Oberlack
Chair of Fluid Dynamics,
Department of Mechanical Engineering
Technical University of Darmstadt
64287 Darmstadt, Germany
oberlack@fdy.tu-darmstadt.de

Yongqi Wang
Chair of Fluid Dynamics,
Department of Mechanical Engineering
Technical University of Darmstadt
64287 Darmstadt, Germany
wang@fdy.tu-darmstadt.de

ABSTRACT

In this work, the focusing of inertial waves emitted by a vertically vibrating torus in a uniformly rotating fluid has been investigated by numerical simulation and theoretical analysis. The primary objective of this study is to explore the localized generation of turbulence around the focal point.

CONTEXT

In the ocean, due to stably stratified fluid, the energy injected by tidal forces at the surface generates some internal gravity waves, which interact with the topography. The transfer of this energy into local turbulence occurs due to a focus of internal gravity waves through two mechanisms (Klymak *et al.*, 2012): wave-topography interaction (remote turbulence) and wave-wave interaction away from the topography (local turbulence). An idealized configuration such as an oscillating torus can reproduce this focus of waves at the apex of the propagation cone with an angle θ (see figure 1). Several studies using internal gravity waves or inertial waves in a rotating fluid have analyzed this torus configuration by using numerical simulations of inertial waves (Duran-Matute *et al.*, 2013), experiments of internal gravity waves (Shmakova & Flór, 2019), or the theory of internal gravity waves (Voisin *et al.*, 2011). Based on the theoretical work on an oscillating sphere by Voisin *et al.* (2011), Shmakova & Flór (2019) assumed a preferential angle θ_p at which the amplification of the amplitude in the focal region is maximal for internal gravity waves. At this angle θ_p, the maximum energy of the waves is transferred to the focus zone and could be converted into local

turbulence. The optimal angle θ_p is determined here by using numerical simulation and theoretical analysis.

GOVERNING EQUATIONS

We consider a uniformly rotating fluid with angular velocity $\mathbf{\Omega}$, density ρ and kinematic viscosity ν. For low-amplitude disturbances, the departures of pressure p and velocity $\boldsymbol{u}$ from the undisturbed rotating flow are governed by the linearized equations of motion in the rotating system (Greenspan, 1968)

$$\frac{\partial \boldsymbol{u}}{\partial t} + 2\mathbf{\Omega} \times \boldsymbol{u} = -\frac{1}{\rho}\nabla p + \nu\nabla^2 \boldsymbol{u} + \boldsymbol{f}, \qquad (1)$$

$$\nabla \cdot \boldsymbol{u} = 0. \qquad (2)$$

Here p represents the reduced pressure, which includes the hydrodynamic pressure and the centrifugal force. It is known that inertial wave can be generated in the rotating flow as a result of the restoring action of the Coriolis force. The propagation direction of the wave energy is determined only by the ratio between the forcing frequency ω_f and the rotation rate Ω of the fluid as following (Sagaut & Cambon, 2008)

$$\theta_{IW} = \cos^{-1}(\omega_f/2\Omega). \qquad (3)$$

In this work, by using a vertically oscillating ring of Dirac type to simulate the oscillation of a torus, we force the inertial waves to focus into the apex of the propagation cone (see
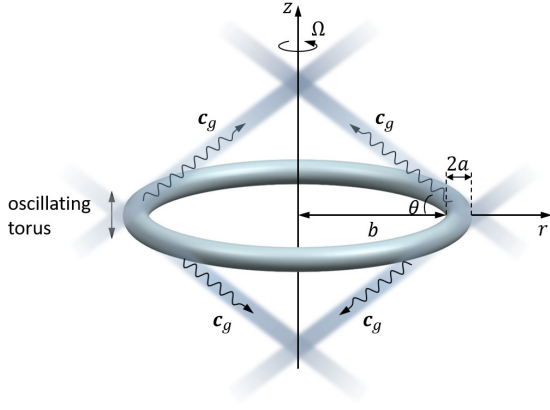
Figure 1.   Schematic drawing of the oscillating torus and the focusing effect of the resulting inertial waves, where a is the radius of the tube and b the major radius of the torus with $a \ll b$, Ω is the constant angular velocity of the rotating flow. c_g denotes the group velocity, at which the wave energy propagates, and θ is the propagation angle.

figure 1).

Several non-dimensional numbers have been used to characterize the oscillation of the torus in a similar way to what has been done in stratified fluid (Ermanyuk *et al.*, 2017): the Keulegan-Carpenter number $Ke = \frac{A}{b}$, which represents the ratio of the forcing amplitude to the minor radius of the torus, the Stokes number $St = \frac{\omega_f b^2}{\nu}$, the Rossby number $Ro = \frac{\omega_f A}{2b\Omega}$ (Davidson, 2013), and the Reynolds number $Re = \frac{\omega_f A \cdot 2b}{\nu}$. We adapt this number in our case of a ring with Dirac-type forcing by changing b into a.

Next, the theoretical analysis and numerical simulation of wave focusing will be presented in detail.

METHODS
Theoretical analysis

Let b, Ω^{-1}, U characterize the typical length, time and relative fluid velocity to the rotating flow. With this, the linearized equation system can be reduced to a dimensionless form. Furthermore, applying the operator $(\frac{\partial^2}{\partial t^2}\nabla\cdot)$ to (1) and taking the continuity equation (2) into account lead to a single wave-like equation for the pressure p in the form

$$\left(\frac{\partial}{\partial t} - Ek\nabla^2\right)^2 \nabla^2 p + (2\boldsymbol{n}\cdot\nabla)^2 p = 4\boldsymbol{n}\cdot(\boldsymbol{n}\cdot\nabla)\boldsymbol{f} +$$

$$2\boldsymbol{n}\cdot\left(\frac{\partial}{\partial t} - Ek\nabla^2\right)(\nabla\times\boldsymbol{f}) + \left(\frac{\partial}{\partial t} - Ek\nabla^2\right)^2 (\nabla\cdot\boldsymbol{f}), \quad (4)$$

where $\boldsymbol{n}$ is a unit vector indicating the direction of the rotation axis. For the following analysis, we define $\boldsymbol{n}$ as the z-axis. The Ekman number $Ek = \frac{\nu}{\Omega b^2}$ is a gross measure of the viscous force compared to the Coriolis force.

In our case, see figure 1, the forcing $\boldsymbol{f}$ has only one component in z-direction, which can be described using the Dirac function in the cylindrical coordinate system as

$$f_z(r,\varphi,z,t) = A\delta(r-1)\delta(z)e^{-i\sigma t}. \quad (5)$$

Here A is a constant line density of the force along the torus, σ is the ratio between the oscillation frequency ω_f of the torus

and the rotation rate Ω of the fluid. This equation can be analytically solved using the Fourier transform. Substituting the solution for p into the momentum equation (1) yields the solution for velocity $\boldsymbol{u}$. The focusing phenomenon caused by the the forcing $\boldsymbol{f}$ is included in the particular solutions, which is the key topic of the present analysis.

Considering the forcing condition (5), the wave-like equation for the pressure (4) in a viscous fluid is given by

$$\left(\frac{\partial}{\partial t} - Ek\nabla^2\right)^2 \nabla^2 p + 4\frac{\partial^2 p}{\partial z^2}$$
$$= \Lambda_0 \left[4 - \left(\sigma - iEk\nabla^2\right)^2\right]\delta(r-1)\delta'(z)e^{-i\sigma t}. \quad (6)$$

Using the Fourier transform in cylindrical coordinate system, we obtain the inhomogeneous solution for the pressure in Fourier space

$$\hat{p}(k_r,k_z,t) = i2\pi\Lambda_0 e^{-i\sigma t}\frac{\left[4 - \left(\sigma + iEk\kappa^2\right)^2\right]k_z J_0(k_r)}{\left(\sigma + iEk\kappa^2\right)^2 \kappa^2 - 4k_z^2}. \quad (7)$$

Additionally, the transformation of the momentum equation (1) in z-direction into Fourier space results in the following scalar equation

$$\left(\frac{\partial}{\partial t} + Ek\kappa^2\right)\hat{u}_z = -ik_z\hat{p} + \hat{f}_z, \quad (8)$$

where $\hat{f}_z = 2\pi\Lambda_0 J_0(k_r)e^{-i\sigma t}$.

Substituting (7) into (8), the inhomogeneous solution of u_z in Fourier space follows as

$$\hat{u}_z = i2\pi\Lambda_0 e^{-i\sigma t}\frac{J_0(k_r)k_r^2\left(\sigma + iEk\kappa^2\right)}{\left(\sigma + iEk\kappa^2\right)^2 \kappa^2 - 4k_z^2}. \quad (9)$$

Applying the Fourier transform in the cylindrical coordinate system to the wave-like equation (4) and then inserting the solution of the pressure p into the momentum equation (1), we obtain the analytical solution of the vertical velocity

$$u_z = e^{-i\sigma t}\frac{\Lambda_0}{2}\int_0^\infty k_r^3 J_0(k_r)J_0(rk_r)\cdot e^{i|z|\alpha f_1}e^{-|z|\alpha f_2} \quad (10)$$
$$\times \frac{[\sigma(4-\sigma^2)f_1 + 4Ek k_r^2 f_2] + i[4Ek k_r^2 f_1 - \sigma(4-\sigma^2)f_2]}{\sigma(4-\sigma^2)^{3/2}(f_1^2 + f_2^2)}dk_r$$

where $\alpha = \frac{\sigma}{\sqrt{4-\sigma^2}}$, and

$$f_{1,2} = \frac{k_r}{\sqrt{2}}\sqrt{\sqrt{\left[1 - \frac{64Ek^2 k_r^4}{\sigma^2(4-\sigma^2)^3}\right]^2 + \frac{1024Ek^2 k_r^4}{\sigma^2(4-\sigma^2)^4}} \pm \left[1 - \frac{64Ek^2 k_r^4}{\sigma^2(4-\sigma^2)^3}\right]}.$$

Numerical simulations

Besides the analysis in the previous section, the governing equations (1) and (2) are solved using the standard pseudo spectral method in a periodic domain with 2π length cube and spatial resolution of 512^3 points.

We perform 25 linear direct numerical simulations DNS by varying the angle of inertial waves propagation to know if there is a propagation angle maximizes the energy in the focus
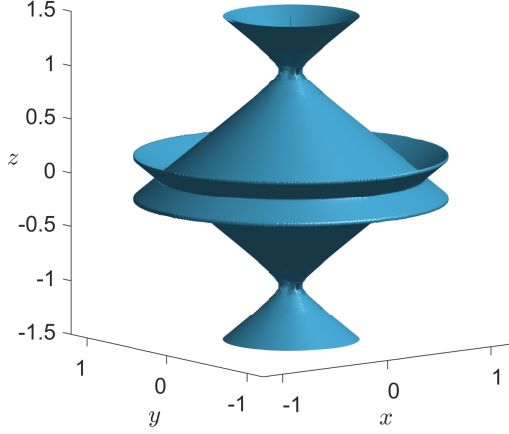
Figure 2. Inertial-wave cone excited by the oscillating dirac torus as depicted by isosurface of u_z according to the analytical solution (10) for inviscid fluid, i.e. Ek= 0.

zone. We keep the viscosity constant $v = 10^{-4}$, the ring radius $a = 1$, the amplitude of forcing $A = 0.01$ and frequency of forcing $\omega_f = 5$, in that case $Re = \frac{\omega_f A \cdot a}{v} = 500$, the Keulegan-Carpenter number $Ke = 0.01 \ll 1$ where the forcing amplitude is assumed to be smaller than the radius b, and the Stokes number $St = 50000 \gg 1$ as a result of the choice of small viscosity. Nevertheless we vary the angle of cone in the range of $\theta = 10°$ to $70°$ by varying the rotating rate $2\Omega_z = 5.077$ to 14.61 and at the same time $Ro = \frac{\omega_f A}{a\Omega}$ varies from 0.019 to 0.0068 (table 1). Note that, inertial waves appear in low Reynolds and low Rossby regime, where in the regime of high Reynolds and low Rossby, waves-turbulence interactions occur according to Godeferd & Moisy (2015).

In the second set of simulations, we perform 5 linear simulations using a solid body with a three-dimensional torus shape. By using a penalisation method as done by Duran-Matute et al. (2013), we force the torus body to oscillate vertically and we vary the propagation angle.

The parameters of this set is chosen to be, the viscosity $v = 10^{-5}$, the amplitude of forcing $A = 0.0157$ and the frequency of forcing $\omega_f = 1.256$. With using torus geometry as following, minor radius of $b = 0.0942$ and major radius $a = 0.848$, by varying the rotating rate $2\Omega_z = 1.996$ to 2.44, we vary the angle θ between $51°$ and $59°$, see table 1. The resulting non-dimensional numbers, i.e. the Reynolds number $Re = 372$, the Rossby number which varies between 0.085 and 0.105, the Stokes number $St = 1115$, and the Keulegan-Carpenter number $Ke = 0.167$.

RESULTS
Viscous spreading on the focus zone

We evaluated the integral with respect to k_r in (10) numerically and plotted the solution. Figure 2 shows the isosurface of u_z for the inviscid case Ek= 0. Figure 3 shows the distribution of the vertical velocity amplitude according to (10) in the vertical plane (r,z) for $\sigma = 1$ and the Ekman number Ek= $0, 10^{-5}, 10^{-4}$ and 10^{-3}, respectively. Due to symmetry, we only present the propagation of the wave beam in one quadrant. The result shows that as the value of the Ekman number increases, the effect of viscous attenuation becomes stronger, which leads to a rapid dissipation of energy during the propagation. As a result, with increasing viscosity the focal zone

becomes increasingly blurred, the amplitude of the waves is greatly reduced and the position of the maximum amplitude of u_z moves in the negative direction of the z-axis.

In order to be able to analyze the viscous effect described in (10) more intuitively, we further simplify it by introducing the assumption of small Ekman number, i.e. $Ek \ll 1$. Using Taylor expansion and neglecting all terms with $\mathcal{O}(Ek^2)$, f_1 and f_2 can be simplified to the following approximations

$$f_1 \approx k_r, \tag{11a}$$

$$f_2 \approx \frac{16Ekk_r^3}{\sigma(4-\sigma^2)^2}. \tag{11b}$$

Correspondingly, the solution of u_z in (10) can be simply expressed as

$$u_z \approx e^{-i\sigma t} \int_0^{\bar{k}_r} A e^{i(|z|\alpha k_r - \psi)} e^{-|z|\alpha\beta k_r^3} dk_r \tag{12}$$

with

$$A = \frac{\Lambda_0 \alpha}{2\sigma} k_r^2 J_0(k_r) J_0(rk_r), \tag{13a}$$

$$\psi = \arctan \frac{4\sigma Ekk_r^2}{(4-\sigma^2)^2}, \tag{13b}$$

$$\beta = \frac{16Ek}{\sigma(4-\sigma^2)^2}. \tag{13c}$$

Here A denotes the amplitude as in the inviscid fluid, ψ represents the phase shift and β a factor of viscous effect. It is to be noted that both ψ and β are affected not only by the viscosity but also by the forcing frequency. The larger ψ and β are, the wider is the wave beam and weaker is the focusing effect.

At the focal point, where $r = 0$ and $|z| = 1/\alpha$, the effect of viscous attenuation is actually dominated by the factor $e^{-\beta k_r^3}$, which decays rapidly as k_r increases. Fig. 4 shows, the exponential function $e^{-\beta k_r^3}$ converges to zero at a smaller wavenumber k_r with increasing value of Ek as well as $\sigma \to 0$ and $\sigma \to 2$. For this we postulate the existence of a cutoff wavenumber $\bar{k}_r$ so that viscous attenuation eliminates all waves with the wavenumbers that are significantly greater than $\bar{k}_r$. In numerical evaluation, an attenuation factor e^{-c} can be predefined, where the constant c is used to control the precision of the integration result. As an example, the choice of $c = 10$ corresponds to an attenuation factor $e^{-c} \approx 4.5 \times 10^{-5}$, which may be sufficiently small for applications. The value of cutoff wavenumber $\bar{k}_r$ of the function $e^{-\beta k_r^3}$ corresponding to the chosen attenuation factor e^{-c} can be reasonably estimated by

$$\bar{k}_r = \left(\frac{c}{\beta}\right)^{1/3} = \left[\frac{c\sigma(4-\sigma^2)^2}{16Ek}\right]^{1/3}. \tag{14}$$

Equation (14) shows that for the same non-dimensional forcing frequency σ, the cutoff wavenumber $\bar{k}_r$ decreases with a scaling proportional to $Ek^{1/3}$. Furthermore, for the same value of Ek, the cutoff wavenumber $\bar{k}_r$ also tends to zero as the $\sigma \to 0$ and $\sigma \to 2$, which corresponds to disappearance of focusing phenomenon.

Fig. 5 shows the change of the amplitude of the vertical velocity at the focal point with the Ekman numbers Ek and the

DNS	$2\Omega_z$	θ	$Ro = \frac{\omega_f A}{(a)\Omega}$
1	5.077	10°	0.019
2	5.32	20°	0.018
3	5.77	30°	0.017
4	6.52	40°	0.0153
5	6.62	41°	0.0151
⋮	⋮	⋮	⋮
24	10	60°	0.01
25	14.61	70°	0.0068

DNS	$2\Omega_z$	θ	$Ro = \frac{\omega_f A}{(b)\Omega}$
26	1.9968	51°	0.105
27	2.088	53°	0.1
28	2.1908	55°	0.095
29	2.307	57°	0.09
30	2.44	59°	0.085

Table 1. Simulation parameters for Linear DNS for ring of Dirac forcing on the left from number 1 to number 25, and solid body torus forcing on the right from number 26 to number 30.
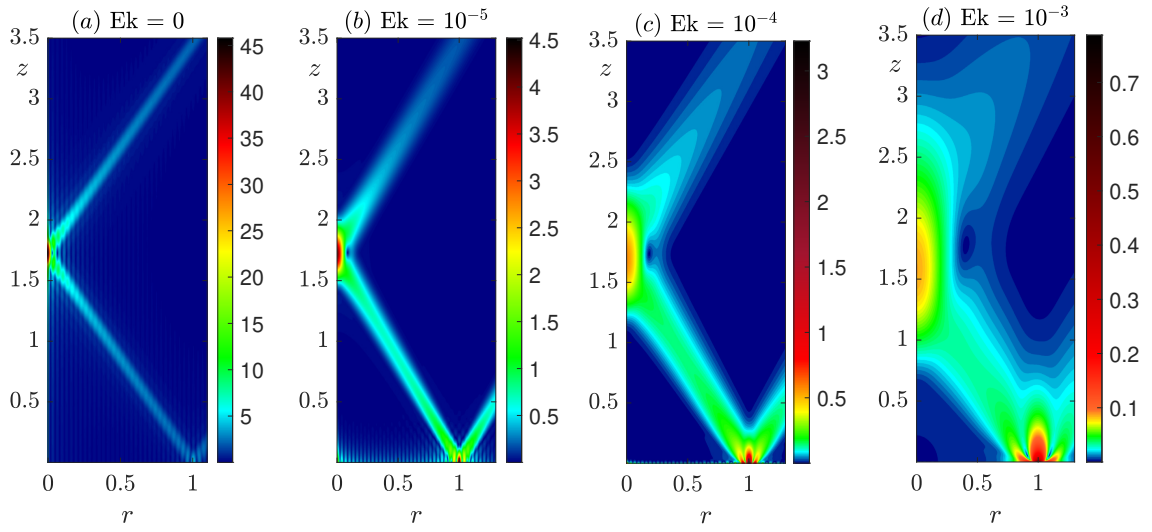

Figure 3. Amplitude of the vertical velocity in the vertical plane according to equation (10) for $\sigma = 1$ in a viscous fluid with the Ekman number (a) Ek= 0, (b) Ek= 0.10^{-5}, (c) Ek= 10^{-4} and (d) Ek= 10^{-3}, respectively.
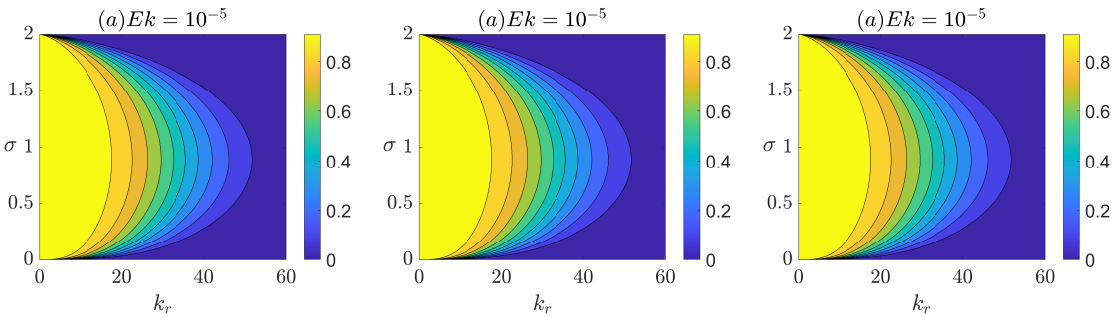

Figure 4. Plot of the function $e^{-\beta k_r^3}$ defined in equation (13c) with the change of σ and k_r for the Ekman number (a) $Ek = 10^{-5}$, (b) $Ek = 10^{-4}$ and (c) $Ek = 10^{-3}$, respectively.

dimensionless forcing frequency σ. It is easy to understand that the focusing phenomenon disappears when σ tends to 0, because in this case the waves propagate in vertical direction along the cylindrical surface on which the oscillating torus is located according to Eq. (3) and thus do not focus on the z-axis. However, the disappearance of wave focusing at $\sigma \to 2$ is limited to the case where the external force is present only in the

z direction. Furthermore, $\sigma \to 2$ corresponds also to the case with an infinitely large viscous effect as described in (13c), so that the energy is rapidly dissipated during propagation and cannot be focused effectively. Additionally, For forcing frequency close to the angular velocity of rotating fluid, i.e. σ is close to 1, the amplitude of the vertical velocity at the focal point reaches its maximum, which corresponds to a wave
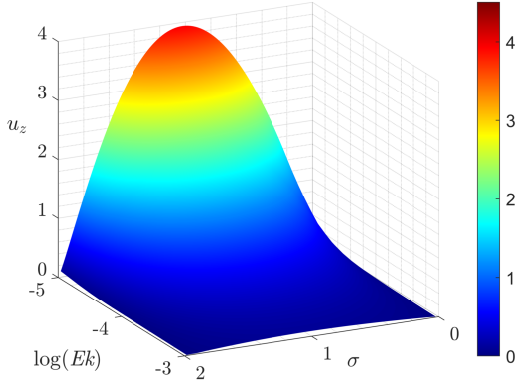
Figure 5. Amplitude of the vertical velocity at the focal point in a viscous fluid with a slight lowering compared its position in an inviscid fluid ($r = 0$, $z = 1/\alpha$) as a function of the dimensionless frequency σ from 0 to 2 and the Ekman number Ek from 10^{-5} to 10^{-3}.

propagation angle slightly less than 60° due to viscous effects. Since the theoretical solution is very complicated, this preferential angle will be further investigated by numerical simulation.

Transfer to vertical velocity

To compare with the theoretical results, we first simulate the vertical velocity distribution. Figure 6 shows a two-dimensional cut of the vertical velocity u_z contour in the vertical plane, where the rays of inertial waves form a double cone with two focal points. This phenomenon is consistent with the theoretical results. Furthermore, for each simulation forced with a vertically oscillating ring of Dirac forcing, we extract the vertical velocity u_z of the focus zone as a function of time. The theoretical position of the focus point is $Z_f = a \cdot \tan(\theta)$, so for each simulation we extract a small cube of the velocities of the theoretical focus point and its neighborhood, the cube has 4 grid cells in each direction. For each point, we obtain the signal of vertical velocity. Extracting the amplitudes and then averaging them, we obtain the amplitude reported on figure 7 for each angle θ. We observe that there is a vertical velocity focusing maximum where the angle $\theta = 55°$ maximizes the vertical velocity at the focus zone. For the case of torus body forcing simulations, the averaged vertical velocity amplitude for each simulation is obtained, and a maximum of the focusing of the velocity is observed in the simulation at $\theta = 57°$.

In the stratified fluid the dispersion relation is given as $\theta_{IGW} = \pm N \sin^{-1}(\omega/N)$, where N is the Brunt–Väisälä frequency, while in the rotating fluid the dispersion relation is $\theta_{IW} = \pm \cos^{-1}(\omega/2\Omega)$ as defined in equation (3). In the work of Shmakova & Flor (2019), it was demonstrated that the angle at which the maximum energy is extracted into the focus zone in the case of a stratified fluid is $\theta_{IGW} = 35°$ for internal gravity wave, so it is coherent to have $\theta_{IW} = \theta_{IGW} - 90°$.

Geostrophic mode

The solution of the vertical velocity using the torus body forcing shows that a stationary geostrophic mode develops in the flow, vertically elongated above and below the torus body, see figure 8. This geostrophic mode is dominating in the mean flow. In the mean flow, we observe two clockwise and counterclockwise rotating cylinders with radius similar to the torus
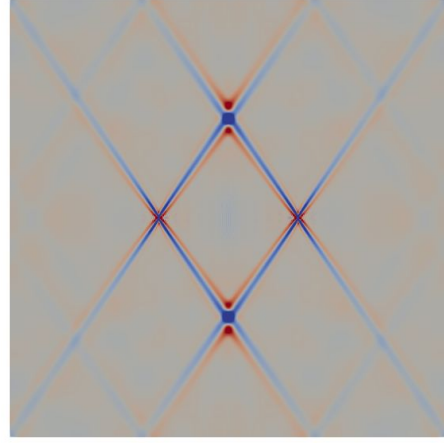

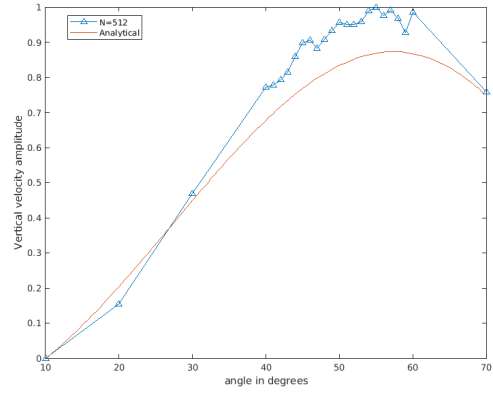Figure 6. 2D cut of the vertical velocity u_z contour from DNS using the parameters number 19 in table 1.

Figure 7. The normalized amplitude of the vertical velocity component u_z in the focus zone as a function in the waves propagation angle θ. Comparison of the analytical solution in (10) for $Ek = 10^{-4}$ with DNS of the parameters from number 1 to number 25 listed in table 1.

major radius. The geostrophic mode appears also in the ocean, where the Coriolis force is balanced by the pressure gradient (Davidson, 2013).

CONCLUSION AND OUTLOOK

Both our analytical and numerical result show that the rays of inertial wave emitted by a vertically vibrating torus form a double cone symmetric about the torus with two focal points, where the wave amplitude has a maximum due to wave focusing. This phenomenon is in good agreement with the experimental and numerical study by Duran-Matute *et al.* (2013). Furthermore, we have analyzed the the effect of viscous spreading on the focus zone. The result shows that as the Ekman number increases, the wave beam becomes wider, the focusing effect becomes weaker, and focus zone moves towards the negative direction of the z- axis compared with the case of an inviscid fluid. Moreover, our numerical simulation shows that the inertial waves are able to extract the maximum energy of focusing at an angle of $\theta_{IW} = 55°$. Based on the results obtained in this work, we are presently analyzing the focusing of inertial waves in the fully nonlinear regime and explore the localized generation of turbulence around the fo-
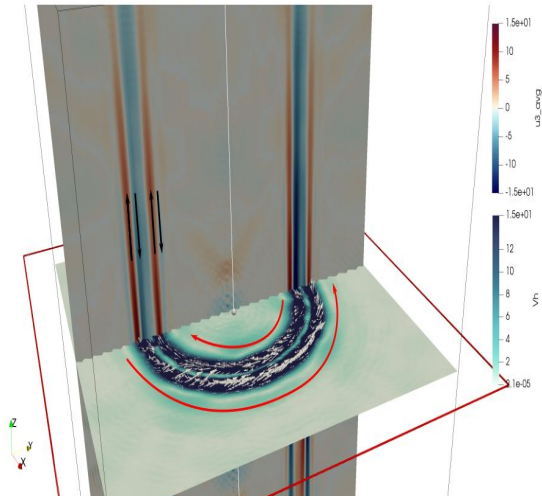
Figure 8.   Vertical averaged velocity on the vertical plane and horizontal averaged velocity on the horizontal plane from DNS using the parameters number 29 in table 1.

cal point.

REFERENCES

Davidson, Peter Alan 2013 *Turbulence in rotating, stratified and electrically conducting fluids*. Cambridge University Press.

Duran-Matute, M., Flór, J.-B., Godeferd, F. S. & Jause-Labert, C. 2013 Turbulence and columnar vortex formation through inertial-wave focusing. *Phys. Rew. E* **87**, 041001(R).

Ermanyuk, Evgeny V, Shmakova, ND & Flór, J-B 2017 Internal wave focusing by a horizontally oscillating torus. *Journal of Fluid Mechanics* **813**, 695–715.

Godeferd, Fabien S & Moisy, Frédéric 2015 Structure and dynamics of rotating turbulence: a review of recent experimental and numerical results. *Applied Mechanics Reviews* **67** (3).

Greenspan, H. P. 1968 *The theory of rotating fluids*. Cambridge University Press.

Klymak, J. M., Legg, S., Alford, M. H., Buijsman, M., Pinkel, R. & Nash, J. D. 2012 The direct breaking of internal waves at steep topography. *Oceanography society* **25**, 041001(R).

Sagaut, P. & Cambon, C. 2008 *Homogeneous turbulence dynamics*. Cambridge University Press.

Shmakova, N. D. & Flór, J.-B. 2019 Nonlinear aspects of focusing internal waves. *J. Fluid Mech.* **862**, R4.

Voisin, B., Ermanyuk, E. & Flór, J. 2011 Internal wave generation by oscillation of a sphere, with application to internal tides. *J. Fluid Mech.* **666**, 308–357.